THE AMERICAN MINERALOGIST, VOL. 56, MARCH–APRIL, 1971

REFINEMENT OF THE CRYSTAL STRUCTURES OF EPIDOTE, ALLANITE AND HANCOCKITE

W. A. DOLLASE, *Department of Geology*
University of California, Los Angeles 90024.

ABSTRACT

Complete, three-dimensional crystal structure studies, including site-occupancy refinement, of a high-iron epidote, allanite, and hancockite have yielded cation distributions $Ca_{1.00}Ca_{1.00}(Al_{0.93}Fe_{0.05})Al_{1.00}(Al_{0.24}Fe_{0.76})Si_3O_{13}H$ for epidote, $Ca_{1.00}(RE_{0.74}Ca_{0.26})(Al_{0.66}Fe_{0.34})Al_{1.00}(Al_{0.17}Fe_{0.83})Si_3O_{13}H$ for allanite, and $Ca_{1.00}(Pb_{0.5}Sr_{0.25}Ca_{0.25})(Al_{0.86}Fe_{0.14})Al_{1.00}(Al_{0.16}Fe_{0.84})Si_3O_{13}H$ for hancockite. These results when combined with those obtained in previous epidote-group refinements establish group-wide distribution trends in both the octahedral sites and the large-cation sites. Polyhedral expansion or contraction occurs at those sites involved in composition change but a simple mechanism, involving mainly rigid rotation of polyhedra, allows all other polyhedra to retain their same geometries in all the structures examined.

INTRODUCTION

As part of a study of the structure and crystal chemistry of the epidote-group minerals, the first half of this paper reports the results of refinement of the crystal structures of three members of this group: allanite, hancockite, and (high-iron) epidote. Also, as an aid in assigning the Fe^{2+}, Fe^{3+} occupancy of the sites in allanite, a preliminary Mössbauer spectral analysis of this mineral is presented. In the second half these structures are compared with three other members of the epidote group that were recently refined, clinozoisite (Dollase, 1968), piemontite (Dollase, 1969), and low-iron epidote (P. Robinson and J.-H. Fang, in preparation). These six structures serve to delineate the major crystalochemical features and variations that occur in these widespread, rock-forming silicates.

The epidote group can be represented by the ideal formula $A_2M_3Si_3O_{13}H$ where the A sites contain large, high-coordination number cations such as Ca, Sr, lanthanides, etc., and the M sites are occupied by octahedrally coordinated, trivalent (occasionally divalent) cations such as Al, Fe^{3+}, Mn^{3+}, Fe^{2+}, Mg, etc. All the members of the group to be discussed here have monoclinic, $P2_1/m$ symmetry.[1]

Besides the original determination of the epidote structure by Ito, reported in 1950, X-ray structural studies of this group have been reported by Belov and Rumanova (1953, 1954); Ito, Morimoto, and Sadanaga

[1] The relationship of the orthorhombic mineral zoisite to the monoclinic epidote mineral of the same composition (clinozoisite) has been detailed previously (Dollase, 1968). A somewhat analogous structural relationship also exists between the mineral ardennite and the epidote structure (Donnay and Allmann, 1968).

(1954); Ueda (1955); Rumanova and Nikolaeva (1959); and Pudovkina and Pyatenko (1963). The first studies were on epidotes of composition near $Ca_2(Al_2Fe_1)Si_3O_{13}H$, while the latter three were studies of allanites wherein rare earth elements replace calcium, and ferrous iron or magnesium is found in octahedral sites in addition to aluminum and ferric iron. These earlier studies served to establish the epidote structure-type and have given some evidence of ordering in both the (two) A sites and (three) M sites.

The early studies, by and large, leaned heavily on two-dimensional Fourier refinement of film-collected data and are not sufficiently accurate to allow unambiguous comparison of the resulting structures. Therefore, refinement of both an epidote from the same locality as used by Ito and an allanite are included here and are considered to supplant these earlier less-precise structure determinations.

In addition to X-ray diffraction studies, the ordering of the transition metals iron and manganese, among the octahedral sites, has been studied by optical absorption spectra (Burns and Strens, 1967) and, in the case of Fe, by Mössbauer spectra (Bancroft, Maddock, and Burns, 1967). The results of these studies have been compared previously with the ordering found by site occupancy refinement of piemontite (Dollase, 1969).

Crystal Structure Refinement of Epidote, Allanite, and Hancockite

Material. All three mineral specimens studied were obtained from the UCLA mineral collection. The Prince of Wales Island, Alaska, locality is well known for its museum-quality epidote specimens. Ito (1950) gave its iron content as 15.53 wt. percent Fe_2O_3 which corresponds to 0.94 Fe atoms per thirteen-oxygen formula unit. Electron microprobe wavelength scans showed minor amounts of Mn, Ti, and Mg in addition to the major elements. Semiquantitative probe data normalized to three octahedral cations leads to $Ca_2(Al_{2.15}Fe^{3+}_{.81}Ti_{.02}Mn_{.02})Si_3O_{13}H$ as the best estimate of composition. Note that this is a lower iron-content than given by Ito. The cell dimensions of this epidote are $a=8.914(9)$, $b=5.640(3)$, $c=10.162(9)$ Å, $\beta=115.4(2)^\circ$ measured from Mo-radiation precession photographs (as were the cell dimensions of the other two minerals given below). Ito (1950) gives $a=8.96$, $b=5.63$, $c=10.30$, $\beta=115.4^\circ$ for the cell dimensions of this epidote. The $P2_1/m$ symmetry of all three minerals was confirmed by the subsequent refinement.

The allanite is from Pacoima Canyon, Los Angeles County, California, where it occurs with zircon and apatite in a pegmatite (Neuerberg, 1954). A partial X-ray fluorescence analysis of this allanite, including determination of calcium, lanthanides, and yttrium content, is given by Frondel (1964). She further shows via X-ray powder diffraction diagrams that this allanite is among the best crystallized (least metamict) of those studied. Electron microprobe analyses were made as part of this study for the other elements found to be present, viz., Fe, Mn, Ti, Mg, Al (Si and H were not determined). Normalizing to one formula unit and including the data of Frondel, the Pacoima Canyon allanite composition can be estimated as

$$(Ca_{1.20}Y_{0.02}La_{0.23}Ce_{0.48}Nd_{0.07})(Al_{1.65}Fe_{1.20}Ti_{0.06}Mn_{0.04}Mg_{0.04})Si_3O_{13}H.$$

The cell dimensions are $a=8.927(8)$, $b=5.761(6)$, $c=10.150(9)$ Å, $\beta=114.77(5)^\circ$. The

hancockite is from Franklin, New Jersey, apparently its only known locality (Palache, 1935). The crystals are minute and poorly formed. A very old chemical analysis (Penfield and Warren, 1899) leads to the probable formula

$$(Ca_{1.17}\overset{+2}{Mn}_{0.17}Pb_{0.47}Sr_{0.21})(Al_{1.95}Fe_{0.88}Mn_{0.10}Mg_{0.07})(Si_{2.95}Al_{0.05})O_{13}H.$$

The unique aspect of its chemistry is the high lead and strontium content. The cell dimensions are $a=8.958(20)$, $b=5.665(10)$, $c=10.304(20)$ Å, $\beta=114.4(4)°$. The estimated errors in the hancockite cell dimensions are large due to the exceedingly weak and diffuse X-ray patterns given by these small and apparently partially metamict crystals. Further indication of the poorer crystallinity of this material was seen during the reflection intensity measurements, where it was noted that the hancockite reflections were broadened to at least twice the width of the reflections of the other two minerals studied here.

Data collection and refinement. Single crystals of the three minerals were selected for intensity measurements which were made on a single-crystal counter diffractometer of the equi-inclination type. Zirconium filtered, molybdenum radiation was employed. All crystals were rotated about their *b*-axes. The crystal sizes used were epidote .03×.05×.06 mm, allanite .04×.08×.08 mm, and hancockite .03×.06×.15 mm. The data were measured up to $(\sin\theta)/\lambda \approx 0.6$. For epidote and allanite essentially all reflections up to this limit were measured, whereas for hancockite, due to the weak diffraction pattern, only the stronger reflections (as judged from the allanite data) were measured. The data were corrected for background *Lp* factors, and absorption. The absorption correction was large only in the case of the lead-bearing hancockite. The linear absorption coefficients are 35.9 cm^{-1} for this epidote, 67.8 for allanite, and 125.5 for hancockite. The number of independent reflections obtained were 947 for epidote, 846 for allanite, and 438 for hancockite.

Full matrix, least-squares refinement was carried out on the three sets of data using the program written by C. T. Prewitt which allows site-occupancy refinement. Initial coordinates were taken from Ito *et al*, (1954) for epidote and from the previously refined piemontite structure for allanite and hancockite. Neutral scattering curves were taken from the compilation of Ibers (1962). Correction of these curves for anomalous dispersion was made using the data of Cromer (1965). Equal weighting was used throughout. All atoms were refined with isotropic temperature factors except the three heaviest atoms, *A*(1), *A*(2), and *M*(3), which were refined with anisotropic temperature factors. The occupancy of the two large *A*-sites and three octahedral *M*-sites were also refined as least-square variables. The final conventional *R*-values are 5.5 percent for epidote, 6.2 percent for allanite, and 5.9 percent for hancockite. The hydrogen atoms were not located here but may be assumed to occupy positions analogous to those found in the clinozoisite and piemontite structures. The refined atomic coordinates of the three structures are given in Table 1. The isotropic, or equivalent isotropic temperature factors, are given in Table 2. Anisotropic coefficients and the thermal vibration amplitudes derived therefrom are listed in Table 3.

Site occupancy refinement procedure. The results of the site-occupancy refinement are given in Table 4. The product of the multiplier and the number of electrons represented by the scattering curve employed is assumed to approximate the true number of electrons per site (this assumes the scattering curve chosen approximates the shape of the true, composite scattering curve). Since this estimate is only a single number, it cannot uniquely furnish the site occupancy when more than two elements (or less than 100 percent occupancy) occurs at a site. It must be stressed, therefore, that the "inferred occupancy" column of Table 4 is interpretation derived from the chemical compositions given previously which

TABLE 1. FRACTIONAL ATOMIC COORDINATES OF PRINCE OF WALES ISLAND EPIDOTE, PACOIMA CANYON ALLANITE AND HANCOCKITE

Atom	Parameter	Epidote	Allanite	Hancockite
A(1)	*x*	0.7562 (2)	0.7585 (4)	0.7639 (9)
	y	.75	.75	.75
	z	.1510 (2)	.1517 (4)	.1559 (8)
A(2)	*x*	.6042 (2)	.5936 (1)	.5898 (2)
	y	.75	.75	.75
	z	.4241 (2)	.4286 (1)	.4124 (2)
Si(1)	*x*	.3396 (3)	.3389 (5)	.3370 (11)
	y	.75	.75	.75
	z	.0473 (2)	.0369 (5)	.0399 (10)
Si(2)	*x*	.6851 (3)	.6866 (5)	.6872 (11)
	y	.25	.25	.25
	z	.2744 (2)	.2799 (5)	.2777 (10)
Si(3)	*x*	.1844 (3)	.1880 (5)	.1758 (11)
	y	.75	.75	.75
	z	.3189 (2)	.3240 (5)	.3119 (10)
M(1)	*x*	0	0	0
	y	0	0	0
	z	0	0	0
M(2)	*x*	0	0	0
	y	0	0	0
	z	.5	.5	.5
M(3)	*x*	.2946 (2)	.3030 (3)	.2903 (6)
	y	.25	.25	.25
	z	.2245 (1)	.2148 (3)	.2190 (5)
O(1)	*x*	.2339 (5)	.2339 (10)	.235 (2)
	y	.9923 (11)	.9892 (18)	.988 (4)
	z	.0410 (4)	.0263 (9)	.040 (1)
O(2)	*x*	.3040 (4)	.3109 (9)	.290 (2)
	y	.9809 (10)	.9679 (18)	.979 (4)
	z	.3554 (4)	.3630 (8)	.342 (1)
O(3)	*x*	.7957 (5)	.7962 (9)	.796 (2)
	y	.0152 (11)	.0144 (17)	.011 (4)
	z	.3382 (4)	.3376 (8)	.347 (1)
O(4)	*x*	.0528 (7)	.0561 (15)	.052 (3)
	y	.25	.25	.25
	z	.1294 (6)	.1306 (13)	.129 (2)
O(5)	*x*	.0417 (7)	.0494 (15)	.038 (3)
	y	.75	.75	.75
	z	.1471 (6)	.1529 (13)	.146 (2)
O(6)	*x*	.0683 (7)	.0674 (14)	.062 (3)
	y	.75	.75	.75
	z	.4078 (6)	.4119 (12)	.407 (3)
O(7)	*x*	.5164 (7)	.5070 (14)	.517 (3)
	y	.75	.75	.75
	z	.1825 (6)	.1779 (13)	.169 (3)

(Continued on next page)

TABLE 1.—(*Continued*)

Atom	Parameter	Epidote	Allanite	Hancockite
O(8)	x	.5281 (7)	.5396 (15)	.524 (3)
	y	.25	.25	.25
	z	.3099 (6)	.3314 (14)	.309 (3)
O(9)	x	.6265 (7)	.6134 (16)	.642 (3)
	y	.25	.25	.25
	z	.0990 (7)	.1037 (14)	.110 (3)
O(10)	x	.0838 (7)	.0858 (15)	.074 (3)
	y	.25	.25	.25
	z	.4298 (6)	.4280 (13)	.422 (3)

have then been divided in such a way as to be consistent with the refined multiplier values and the "sizes" of the sites involved. As an expedient, the relatively minor Mn, Ti, and Mg contents have been included in the "Fe" estimate in Table 4.

An obvious test of the occupancy refinement is a comparison of the sums of the site occupancies with the previously determined (wet chemical or microprobe) analysis. This comparison is made in the fifth and sixth columns of Table 4. It can be seen that the only serious disagreement is in the case of the *A*-site of allanite, where perhaps the total lanthanide content of the particular allanite crystal studied here is slightly greater than the average obtained *via* fluorescence analysis (Frondel, 1964).

TABLE 2. ISOTROPIC TEMPERATURE FACTORS OF PRINCE OF WALES ISLAND EPIDOTE, PACOIMA CANYON ALLANITE AND HANCOCKITE

Atom	Epidote	Allanite	Hancockite
A(1)[a]	0.76 Å²	1.0 Å²	1.0 Å²
A(2)[a]	.92	.7	1.1
Si(1)	.41 (4)	.7 (1)	0.9 (2)
Si(2)	.48 (4)	.7 (1)	1.1 (2)
Si(3)	.42 (4)	.6 (1)	1.0 (2)
M(1)	.51 (6)	.6 (1)	0.9 (2)
M(2)	.43 (7)	.6 (1)	0.7 (3)
M(3)[a]	.42	.9	0.6
O(1)	.70 (7)	1.3 (2)	1.1 (3)
O(2)	.63 (7)	1.1 (1)	1.1 (3)
O(3)	.79 (7)	1.0 (1)	1.6 (3)
O(4)	.6 (1)	1.2 (2)	0.5 (5)
O(5)	.6 (1)	1.2 (2)	1.1 (5)
O(6)	.5 (1)	0.9 (2)	0.9 (5)
O(7)	.6 (1)	1.0 (2)	1.7 (5)
O(8)	.9 (1)	1.5 (2)	1.8 (5)
O(9)	1.0 (1)	1.7 (2)	1.5 (5)
O(10)	0.7 (1)	1.2 (2)	1.5 (5)

[a] Equivalent isotropic temperature factor.

TABLE 3. ANISOTROPIC THERMAL PARAMETERS AND ELLIPSOIDS

		Epidote	Allanite	Hancockite
(a) Anisotropic coefficients $\times 10^4$				
$A(1)$	β_{11}[a]	37 (3)	59 (6)	52 (13)
	β_{22}	55 (11)	75 (17)	61 (45)
	β_{33}	23 (2)	40 (9)	49 (10)
	β_{13}	18 (2)	31 (4)	43 (9)
$A(2)$	β_{11}	36 (3)	21 (2)	37 (3)
	β_{22}	103 (12)	75 (5)	136 (14)
	β_{33}	14 (2)	11 (1)	33 (3)
	β^{13}	5 (2)	3 (1)	27 (2)
$M(3)$	β_{11}	16 (2)	22 (4)	25 (9)
	β_{22}	30 (8)	69 (13)	85 (3)
	β_{33}	12 (1)	32 (3)	32 (7)
	β_{13}	4 (1)	7 (3)	22 (6)
(b) Axial vibration amplitudes (Å) of thermal ellipsoids				
$A(1)$	1[b]	0.11 (0)	0.11 (2)	0.07 (5)
	2	.10 (1)	.11 (1)	.10 (4)
	3	.08 (1)	.15 (1)	.16 (1)
$A(2)$	1	.12 (1)	.09 (1)	.08 (1)
	2	.13 (1)	.11 (0)	.15 (1)
	3	.08 (1)	.07 (0)	.13 (0)
$M(3)$	1	.08 (1)	.09 (1)	.06 (4)
	2	.07 (1)	.11 (1)	.12 (2)
	3	.07 (0)	.12 (1)	.12 (1)

[a] Of the form $(h^2\beta_{11} + \cdots 2hk\beta_{13} \cdots)$. For these atoms $\beta_{12} = \beta_{23} = 0$.
[b] Axis no. 1 most nearly parallels crystallographic a axis, etc.

Mössbauer spectral analysis of allanite. Although the X-ray results enable a relatively unambiguous distinction between octahedral occupancy by aluminum atoms on the one hand and (Fe, Mn) on the other, site occupancy refinement does not distinguish between Fe^{2+}, Fe^{3+}, Mn^{3+}, Mn^{2+}. Any of these species may be present and unequally distributed between the $M(1)$ and $M(3)$ sites. Fortunately, some information on the iron distribution and valence state in the mineral can be obtained from analysis of its gamma ray resonance absorption spectrum (Mössbauer effect). Mössbauer spectral analyses of a piemontite (octahedral site composition: $Al_{2.04}Fe_{0.33}Mn_{0.63}$) and two epidotes, ($Al_{2.13}Fe_{0.87}$) and ($Al_{2.16}Fe_{0.84}$), have been reported by Bancroft, Maddock, and Burns (1967). They interpreted the spectra as resulting from Fe^{3+} in one and the same site in all three minerals. They estimated that contributions to the spectrum of less than 5 percent of the total intensity would not be resolved.

TABLE 4. LEAST-SQUARES ESTIMATE OF SCATTERING-CURVE MULTIPLIERS AND INFERRED SITE OCCUPANCIES

Crystal	Site	Scat. curve	Multiplier	No. of *e* per site	No. *e* from chem. analysis	Inferred atomic occupancy[a]
Epidote	*A*(1)	Ca	0.98 (1)	19.7 (2)		$Ca_{1.00}$
	A(2)	Ca	0.99 (1)	19.7 (2)		$Ca_{1.00}$
	M(1)	Al	1.048 (15)	13.6 (2)		$Al_{0.93}Fe_{0.05}$
	M(2)	Al	0.98 (1)	12.7 (2)		$Al_{1.00}$
	M(3)	Fe	0.882 (8)	22.9 (2)		$Al_{0.24}Fe_{0.76}$
	Σ*M*			49.2 (4)	49.95	
Allanite	*A*(1)	Ca	1.06 (2)	21.2 (5)		$Ca_{1.00}$
	A(2)	Ce	0.830 (11)	48.2 (6)		$Re_{0.74}Ca_{0.26}$
	Σ*A*			69.4 (8)	65.40	
	M(1)	Al	1.34 (3)	17.4 (4)		$Al_{0.66}Fe_{0.34}$
	M(2)	Al	0.97 (3)	12.7 (4)		$Al_{1.00}$
	M(3)	Fe	0.913 (17)	23.7 (4)		$Al_{0.17}Fe_{0.83}$
	Σ*M*			53.8 (7)	55.45	
Hancockite	*A*(1)	Ca	0.96 (4)	19.2 (7)		$Ca_{1.00}$
	A(2)	[b]	1.03 (2)	57.0 (12)		$Pb_{0.5}Sr_{0.25}(Ca, Mn)_{0.25}$
	Σ*A*			76.2 (14)	74.69	
	M(1)	Al	1.14 (5)	14.8 (6)		$Al_{0.86}Fe_{0.14}$
	M(2)	Al	0.95 (4)	12.3 (6)		$Al_{1.00}$
	M(3)	Fe	0.92 (3)	23.9 (7)		$Al_{0.16}Fe_{0.84}$
	Σ*M*			51.0 (11)	51.57	

[a] See text for details.
[b] $(Pb_{0.5}Sr_{0.25}Ca_{0.25})$.

As part of this study, a Mössbauer spectrum was obtained on a sample of Pacoima Canyon allanite. The methods employed in the data measurement, reduction, and interpretation are those described by Ernst and Wai (1970). Figure 1 is a plot of the experimental data and the fitted spectra. The spectrum can be seen to be complex and consist of more than one doublet; *i.e.*, more than one site and/or oxidation state is involved. From the X-ray data the maximum number of doublets expected

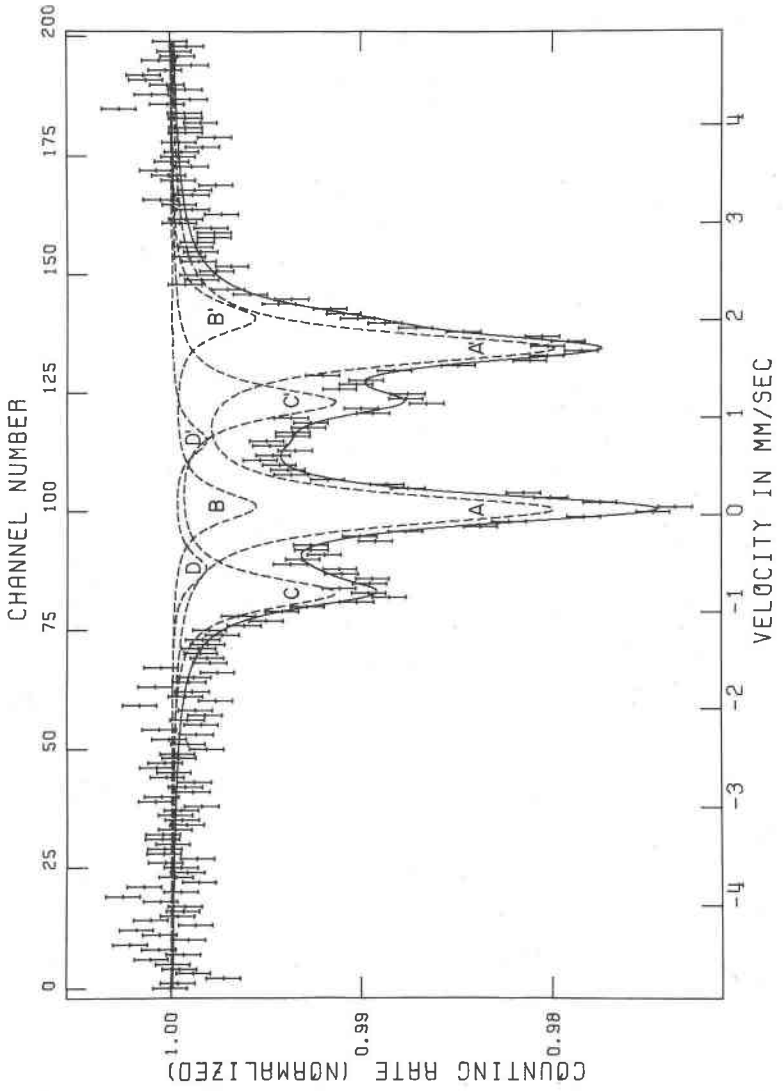

FIG. 1. Observed and fitted Mössbauer spectra of Pacoima Canyon allanite.

is four, attributable to Fe^{2+} in $M(1)$, Fe^{2+} in $M(3)$, and Fe^{3+} in $M(1)$ and Fe^{3+} in $M(3)$. Accordingly, a four-doublet fit to the experimental data was first made and the numerical results given in Table 5. These calculated spectra are also shown in Figure 1. Line pair DD' is so weak as to be of questionable existence, and consequently an attempt was made to fit a three line-pair spectrum to the observed data. The estimate of the fractions of the total intensity attributable to each of the doublets A, B, and C were not significantly changed, however, and the four line-pair spectrum was retained. Probable assignment of doublets can be made from the known variation of isomer shift and quadrupole splitting as a function of valence state and site distortion (see *e.g.*, Ingalls, 1964; Danon, 1968). From the magnitude of the isomer shift, lines A and B can be

TABLE 5. RESULTS OF MÖSSBAUER ANALYSIS OF PACOIMA CANYON ALLANITE

Line-pair	Isomer shift[a]	Quadrupole splitting (mm/sec)	% of total intensity (mm/sec)	Line hwhm (mm/sec)	Interpretation
A	1.07 (3) mm/sec	1.66 (4)	57.3 (2.3)	0.20 (2)	Fe^{2+} in $M(3)$
B	1.24 (15)	1.93 (21)	12.8 (3.5)	0.20 (2)	Fe^{2+} in $M(1)$
C	0.37 (1)	1.97 (3)	24.7 (1.7)	0.20 (2)	Fe^{3+} in $M(3)$
D	0.29 (7)	1.33 (12)	5.3 (1.5)	0.20 (2)	Fe^{3+} in $M(1)$

[a] Relative to metallic iron = 0.0 mm/sec.

attributed to Fe^{2+} in octahedral coordination and lines C and D to Fe^{3+} in octahedral coordination. The larger quadrupole splitting of the B line suggests the *less* distorted site, *viz.* $M(1)$, whereas the larger quadrupole splitting of the Fe^{3+} line, line C, is attributable to Fe^{3+} in the *more* distorted $M(3)$ site. The quadrupole splitting and isomer shift of line-pair CC' is similar to those of the single line-pair reported by Bancroft *et al.*, (1967) for the epidotes and piemontite. If the above assignment is correct, $70(\pm 3)$ percent of the total iron in the allanite is in the ferrous state, and the remaining $30(\pm 3)$ percent is in the ferric state. Applied to the microprobe analysis of 1.20 Fe atoms per formula unit, this yields 0.84 Fe^{2+} and 0.36 Fe^{3+}. The number of Fe^{2+} ions should balance the number of rare-earth atoms replacing calcium which, from the Frondel analysis, total 0.80 atom per formula unit. The internal consistency here, then, is good.

The consistency after dividing the total iron into the two sites is less satisfactory. From the percentages given in Table 5, the $M(3)$ site should contain 0.69 Fe^{2+}, 0.30 Fe^{3+} or 0.99 total Fe atom, whereas the site

refinement yielded only 0.83 "Fe" atom in this site. The $M(1)$ site from the Mössbauer results should contain 0.15 Fe^{2+} and 0.06 Fe^{3+} or 0.21 Fe atom total, whereas the site refinement gave 0.34 "Fe" atom. The site refinement values in addition include a total of 0.10 non-iron atoms which would not appear in the Mössbauer results. The discrepancy between the Mössbauer and site-occupancy refinement values could be due to errors in all three of the experimental methods employed in arriving at these numbers as well as the possibility of compositional variation amongst the allanite grains studied. The site occupancy values for allanite have an estimated standard deviation of 0.03 Fe atoms per site. The percentage of the total number of iron atoms giving rise to each Mössbauer doublet have estimated errors of two to four percent or 0.02—0.05 Fe atoms. The errors in the microprobe analysis can be estimated as perhaps 0.05 Fe atom per formula unit. The observed discrepancies would then be near the maximum error expected.

The fact that the Mössbauer values lead to essentially complete occupancy of the $M(3)$ site by iron atoms, whereas the allanite, hancockite, piemontite, and epidote refinements all yielded about 85 percent Fe+Mn occupancy of this site, makes the Mössbauer values seem more suspect. Since the Mössbauer derived total Fe^{2+} vs Fe^{3+} values were consistent with the other chemical data and since the Mössbauer values lead to too much Fe in $M(3)$ and too little in $M(1)$, it seems likely that the error lies in the division of ferrous iron between $M(1)$ and $M(3)$. As the isomer shift and quadrupole splitting of lines AA' and BB' are similar, the precision of separating these pairs is low. For these reasons it is, therefore, suggested that the Mössbauer derived Fe^{2+} content of $M(3)$ should be reduced by perhaps 0.10 atom and that of $M(1)$ increased by this amount, thereby bringing the Mössbauer values more nearly in line with what are thought to be the more correct site occupancy totals.

In summary, further work is needed in order to clear up these discrepancies between the Mössbauer and site occupancy refinement values, and the apparent discrepancy between the isomer shift values. At this stage the Mössbauer data can be taken as at least consistent with the overall Fe^{2+}/Fe^{3+} ratio suggested from charge balance arguments. The data further suggest that iron in both valence states is distributed unequally over two different structural sites.

The fact that Bancroft *et al.*, (1967) obtained only a single line-pair Mössbauer spectrum from the epidotes and piemontite investigated would say that the 0.33 to 0.86 Fe atom per formula unit was restricted to the $M(3)$ site in his samples. However, since Fe^{3+} in the $M(1)$ site yields (in allanite, at least) a doublet only slightly shifted and somewhat less split than the doublet attributable to Fe^{3+} in $M(3)$, it seems likely

that as much as .05 to .10 Fe^{3+} atom in $M(1)$ would merely widen the observed "single" line-pair but remain otherwise undetected.

Crystal Chemistry of the Epidote-Group Minerals

Besides the refinement results presented above, three additional recent epidote group refinements have furnished the following estimates of site occupancies: clinozoisite $Ca_2(Al_{1.00})(Al_{1.00})(Al_{0.96}Fe_{0.04})Si_3O_{13}H$ (Dollase, 1968), lowiron epidote $Ca_2(Al_{1.00})(Al_{1.00})(Al_{0.70}Fe_{0.30})Si_3O_{13}H$ (P. Robinson and J.-H. Fang, in prep.), and piemontite $Ca_{1.00}(Ca_{.87}Sr_{.13})(Al_{.80}M_{.20})$-$(Al_{1.00})(Al_{0.17}M_{.83})Si_3O_{13}H$ where $M=(Mn^{+3}_{.7}Fe^{+3}_{.3})$ (Dollase, 1969). In these formulae the A and M sites are given in their serial order, and the reader is referred to the individual papers for discussion of the bases of these estimates. Bond lengths or other geometrical aspects of these structures considered germane to this paper are reproduced here; for other data the original articles must be consulted.

Description of the epidote structure type. The basic epidote structure type has been described and discussed previously (Dollase, 1968). The polyhedral connectivity is shown in Figure 2. Briefly, the structure contains chains of edge-sharing octahedra of two types: a single chain of $M(2)$ octahedra and a multiple or zig-zag chain composed of central $M(1)$ and peripheral $M(3)$ octahedra. The chains are crosslinked by SiO_4 groups and Si_2O_7 groups. Finally, there remain between the chains and crosslinks relatively large cavities which house the $A(1)$ and $A(2)$ cations.

In order to compare the six structures, the shapes and sizes of the individual coordination polyhedra are first compared. As a second step, changes in the orientation of the polyhedra are discussed. Inasmuch as the differences between the six mineral structures under discussion involve differences in the occupancies of only some of the sites (specifically $A(2)$, $M(1)$, and $M(3)$), it would be expected that there would be major differences in the coordination polyhedra surrounding these sites and that these differences would, in turn, result in only minor secondary modifications or mere rotation-translation of the connecting polyhedra. This expectation is largely borne out.

SiO_4 tetrahedra. Si(1) and Si(2) share O(9), forming an Si_2O_7 group, while Si(3) forms an isolated SiO_4 group. Each tetrahedron retains essentially its same shape and size in all six structures. The different Si-O bond lengths in this structure type, averaged over the six minerals, are given in Table 5 along with the range of lengths encountered (both excluding and including the imprecise hancockite). Statistically, all deviations of individual bond-lengths from their respective weighted averages are less

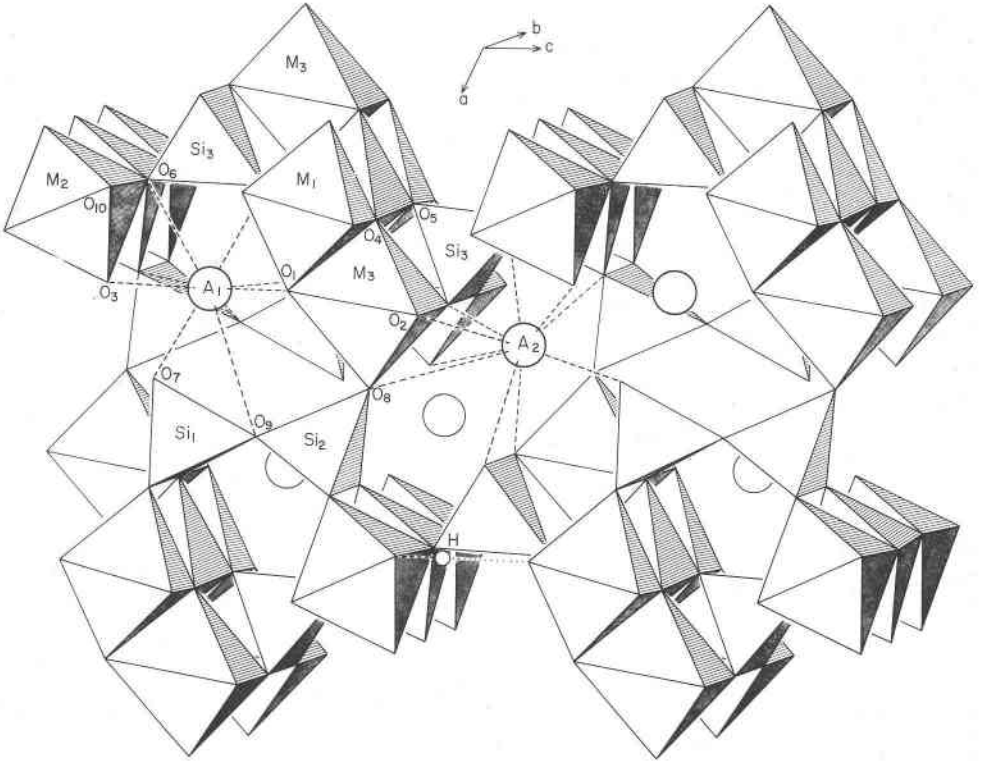

FIG. 2. Polyhedral linkage in the epidote-group minerals.

than twice the bond-length standard deviations (see Table 6), implying the differences are insignificant.

Although in a given bonding situation a particular Si-O bond type has nearly the same value in each of these minerals, the different Si-O bond types have rather widely different lengths (see Table 6). A case has been previously made (Dollase, 1968) relating the bond-length variations in this structure-type to local charge imbalance (Zachariasen valence-balancing). The near uniform length of a given bond in all six structures is consistent with this concept since the degree of local charge imbalance is primarily a result of the topology and therefore is essentially the same in all these structures.

The O-Si-O angles in the Si_2O_7 group are all within 4° of the ideal tetrahedral angle (109.5°). The Si(3) tetrahedron, on the other hand, is somewhat distorted due probably to the fact that it shares it O(2)-O(2′) edge

TABLE 6. WEIGHTED[a] AVERAGE Si–O BOND LENGTHS

	Bond	Length	Range[b]	Range
(2×)	Si –O(7)	1.649 Å	.010 Å	.025 Å
	–O(7)	1.577	.020	.047
	–O(9)	1.635	.027	.027
	Avg.	1.628		
(2×)	Si(2)–O(3)	1.622	.020	.033
	–O(8)	1.598	.020	.039
	–O(9)	1.627	.007	.025
	Avg.	1.617		
(2×)	Si(3)–O(2)	1.623	.026	.030
	–O(5)	1.663	.014	.028
	–O(6)	1.651	.022	.045
	Avg.	1.640		

[a] Weighted inversely proportional to estimated standard deviations of Si–O bond lengths which are 0.006 Å clinozoisite, 0.007 epidote and piemontite, .015 low-iron epidote and allanite, and 0.02–0.03 hancockite.

[b] Excluding hancockite.

with the $A(2)$ polyhedron and the opposite O(5)-O(6) edge with the $A(1)$ polyhedron. The shared edges are somewhat compressed. In the six structures the O(5)-Si-O(6) angle lies in the range 100–103°, and, in addition, in allanite the O(2)-Si-O(2′) angle is compressed to 103°. This latter angle is compressed only in the allanite case, probably due to the face that in this mineral $A(2)$ is occupied mainly by trivalent lanthanide elements and the $A(2)$-Si(3) distance is here the shortest (3.32 Å).

The degree of flexing of the Si_2O_7 group, i.e., the Si(1)-O(9)-Si(2) angle, shows significant variation in the different structures and appears to be directly related to the solid-solution-caused expansion of the connected M(3) octahedron, as discussed below. Recently Brown, Gibbs, and Ribbe (1969) have documented a prediction by Cruikshank (1961) that, *inter alia*, Si-O bond lengths (to shared oxygens) should vary inversely with the Si-O-Si′ angle due to the dependence of the Si-O π-bond order on this angle. Although it is only marginally significant here, due to the size of the bond-length estimated standard deviations, such a trend seems to occur. The Si-O-Si angle decreases more or less regularly from 164° in clinozoisite to 145° in allanite, while the average silicon-to-

bridging-oxygen bond increases from 1.627 Å in clinozoisite to 1.639 in allanite. The other members are within experimental error of this inverse linear relationship.

MO_6 octahedra. One of the most interesting aspects of this structure-type is the markedly unequal occupancy of the three different octahedral positions (herein labeled $M(1)$, $M(2)$, and $M(3)$. Reference to the site occupancies given in Table 4 and the structural formulae reproduced above show that in all six structures, as closely as can be determined, the $M(2)$ octahedral chain contains only aluminum atoms with the non-Al octahedral atoms substituting entirely into the other, $M(1)$-$M(3)$, composite octahedral chain (even though these parallel chains have the same periodicity).

Within the $M(1)$-$M(3)$ chain the occupancy is also non-uniform. In all cases the peripheral $M(3)$ octahedra contain a larger fraction of the non-aluminum atoms (principally Fe and Mn) than the central $M(1)$ octahedra. In the case of clinozoisite and low-iron epidote, the small amount of iron present is found entirely in the $M(3)$ site. (It should be pointed out that site occupancy of the low-iron epidote was not refined by Robinson and Fang; however, the temperature factors associated with the octahedral sites are all reasonable when the iron present is assigned to the $M(3)$ site.)

The remaining epidote minerals show substitution of (Fe,Mn) into both $M(3)$ and $M(1)$ with a maximum of 34 percent of the latter site being so replaced in allanite. This substitution into $M(1)$ occurs even though the $M(3)$ site is not completely occupied by (Fe,Mn). (The maximum amount of (Fe,Mn) substitution into the $M(3)$ site in the cases studied here is *ca.* 85 percent with Al occupying the remaining 15 percent.) More iron or manganese-rich epidote—such as those reported by Strens (1966) with (Fe+Mn)/(Fe+Mn+Al) nearly 0.5—probably have the additional Fe,Mn atoms occurring in the $M(1)$ site.

The size of the octahedra (for convenience, the metal-oxygen bond length averaged over the octahedron) reflects the occupancies as shown in Figure 3. The dashed lines give the slopes that could be ideally expected from the sizes of the ions concerned (Shannon and Prewitt, 1969). There is a rough agreement between the observed rate of increase and that predicted from the ionic radii of Fe^{3+} and Mn^{3+}. In the case of allanite, where much of the iron is in the ferrous state, the average $M(3)$-O bond length is close to the ideal curve drawn for Fe^{2+} replacing Al.

Note that there is an inherent "size" difference between the octahedra with the $M(3)$-O bond length average about .06 Å greater than the

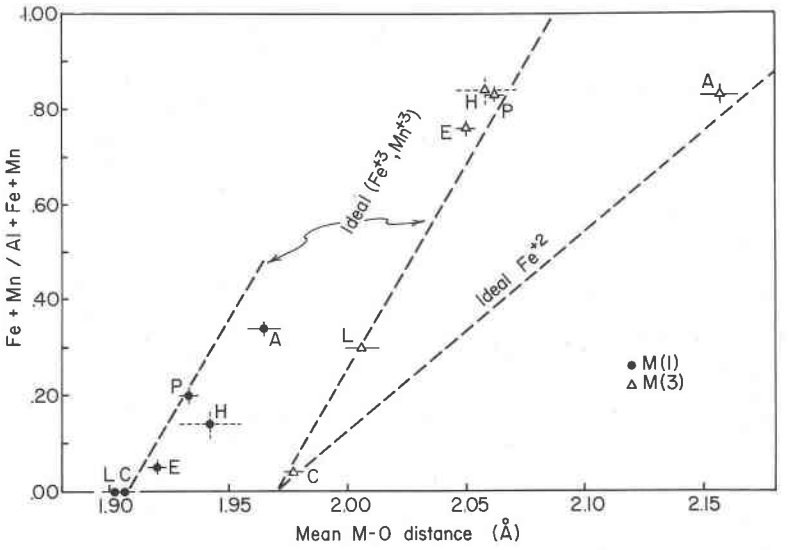

FIG. 3. Trends of metal-oxygen distances in octahedra as a function of site occupancy.

$M(1)$-O average and that this difference is roughly maintained with substitution. The non-random distribution of the cations on the three octahedral sites probably results from both the preference of the Al (over the transition metals, Fe and Mn) for the OH-coordinated $M(2)$ site and the preference of the transition metals (over Al) for the larger and more distorted $M(3)$ site.

The $A(1)$ and $A(2)$ polyhedra. Clinozoisite, low-iron epidote, and epidote have both the large A sites occupied entirely by calcium atoms. In the other three members the calcium atoms are partially replaced by other divalent atoms such as strontium and lead or trivalent lanthanide elements. As with the octrahedral sites, this substitution is markedly non-uniform, and, in fact, all of the atoms replacing calcium are found only in the $A(2)$ site—none in the $A(1)$ site. (See Table 4).

This behavior can be at least rationalized by noting that the substitution is by atoms larger than calcium and that the $A(2)$ site is larger and has a higher coordination number than the $A(1)$ site even when both are completely occupied by calcium atoms.

Considering A-O bonds greater than 3.1 or 3.2 Å as inconsequential, the $A(1)$ site in all cases is 9-coordinated, and the $A(2)$ site is 10-coordinated in all cases except for allanite where this latter site is mostly occupied by lanthanides and an eleventh neighbor at 3.13 Å should

perhaps be included. The size and shape of the $A(1)$ polyhedron in the various members investigated are quite similar. The changes in individual bond lengths in the different minerals are minor. In contrast, the size and shape of the $A(2)$ polyhedron in the six compounds is much more variable, no doubt due to the diverse occupancy of this site. The largest changes involve $A(2)$-O(2) and $A(2)$-O(10) which have values of 2.53–2.57 Å when $A(2)$ is occupied by calcium but 2.88–2.78 Å in hancockite where this site contains largely lead and strontium.

Reorganization. Finally, it is worth examining how this structure type absorbs major changes in site occupancy with the concomitant major expansion or contraction of the coordination polyhedron involved. Evidently the structural change is not a homogeneous expansion or contraction of the entire unit cell since some polyhedra, *e.g.*, the SiO_4 groups, remain the same size in all the structures. Rather, comparison of the atomic coordinates furnished by these different refinements shows that the reorganization of the structure can be largely described by major rotations and minor translations of polyhedra (or groups of polyhedra) which behave as rigid units.

Where polyhedra share edges (such as the $M(1)$-$M(3)$ composite chain) the expansion of one polyhedron necessitates the expansion of (at least one edge of) the connected polyhedron, but there is little rotational reorientation between the two units. On the other hand, where only a corner is shared (such as between $M(3)$ and Si(2) polyhedra) there is a possibility for rotation of one unit relative to the other which may or may not change the M-O-M' angle. In the epidote series this rotation of polyhedra is a prominent aspect of the structural difference between the members. This can be illustrated by reference to Figure 2. If an aluminum ion in $M(3)$ (clinozoisite) is replaced by a Fe^{2+} ion (as in allanite), the $M(3)$ octahedron expands, and specifically the O(8) atom moves away from the $M(3)$ ion. Si(2) tetrahedron has O(8) for one corner and since the Si(2) tetrahedron has the same shape and size in clinozoisite as it has in allanite, then the entire tetrahedron must be translated or rotated (or some combination of both) in going from the clinozoisite structure to the allanite structure. Furthermore, the Si(2) tetrahedron is connected in turn to the $M(2)$ octahedron which also becomes reoriented by the rotation/translation of the Si(2) tetrahedron, and so forth, around any of the numerous circuits that can be drawn using the polyhedral edges. Since reorientation of polyhedra often involves altering bond angles across the polyhedral corners (oxygens) or longer range interactions and since each polyhedron belongs to several such circuits, the net resultant reorientation is not simply predictable.

Some simplification, however, can be seen when, for example, the circuit considered is approximately planar, in which case the sense of rotation (about an axis normal to the circuit) of adjacent polyhedra would not be expected to be the same. Thus, by way of example, a circuit of 14 polyhedra whose centers are at $b \approx \frac{1}{4}$ to $\frac{1}{2}$ consists of $M(3)$-Si(2)-$M(2)$-Si(3)-$M(1)$-Si(1)-Si(2)-$M(3)$-$M(1)$-Si(3)-$M(2)$-Si(2)-Si(1)-$M(1)$ and then repeats. In going from the clinozoisite structure to the allanite structure, the $M(3)$ octahedral expansion initiates the rotations. Starting with the Si(2) tetrahedron, the rotations (which are primarily about the b axis) are $+11°$, $-4°$, $0°$, $+4°$, $-6°$, $+11°$, $-1°$, $+4°$, $0°$, $-4°$, $+11°$, $-6°$, $+4°$, $-1°$, in order. Because there are also translations of the polyhedra involved as well as the overall expansion of the $M(3)$ and $M(1)$ octahedra, the magnitudes of the successive rotations are not the same, but the sense of rotations is seen to alternate or result in a net rotation of zero for some ployhedra.

Structural changes among isomorphous or closely related compounds by this rotation mechanism are probably common and, for example, have been well documented in the so-called tetrahedral layer of layer silicates by Bailey (1966) and others.

Acknowledgments

It is a pleasure to thank Mr. Paul Robinson and Dr. Jen Fang for providing the unpublished results of their low-iron epidote refinement, Mr. Michel Semet for supplying the allanite Mössbauer spectrum, and Mr. Hsing-Chi Chang for assistance in the data collection and microprobe analyses. This research was supported by grants from the Alfred P. Sloan Foundation and the National Science Foundation (GA-1668).

References

Bailey, S. W. (1966) The status of clay mineral structures. *Clays Clay Mineral. Proc. Nat. Conf.* **14**, 1–23.

Bancroft, G. M., A. G. Maddock, and R. G. Burns (1967) Application of the Mössbauer effect of silicate mineralogy: I. Iron silicates of known crystal structure. *Geochim. Cosmochim. Acta* **31**, 831–834.

Belov, N. V. (1954) The crystal structure of epidote. *Trudy Inst. Kristallogr., Akad. Nauk. SSSR*, **9**, 103–164. [Abstr. in *Struct. Rep.* **18**, 544–545 (1900).]

———, and I. M. Rumanova (1953) The crystal structure of epidote $Ca_2Al_2FeSi_3O_{12}(OH)$. *Dokl. Akad. Nauk. SSSR*, **89**, 853–856. [Abstr. in *Struct. Rep.* **17**, 567–568 (1900).]

Brown, G. E., G. V. Gibbs, and P. H. Ribbe (1969) The nature and the variation in length of the Si-O and Al-O bonds in framework silicates. *Amer. Mineral.* **54**, 1044–1061.

Burns, R. G., and R. G. J. Strens (1967) Structural interpretation of polarized absorption spectra of the Al-Fe-Mn-Cr epidotes. *Mineral. Mag.* **36**, 204–226.

Cromer, D. T. (1965) Anomalous dispersion corrections computed from self-consistent field relativistic Dirac-Slater wave functions. *Acta Crystallogr.* **18**, 17–23.

Cruickshank, D. W. J. (1961) The role of 3d-orbitals in π-bonds between (a) silicon, phosphorus, sulfur, or chlorine and (b) oxygen or nitrogen. *J. Chem. Soc.* **1961**, 5486–5504.

DANON, J. (1968) Fe: metal, alloys, and inorganic compounds. *In* V. I. GOLDANSKII AND R. H. HERBER (eds.) *Chemical Applications of Mössbauer Spectroscopy*, Academic Press, N. Y., p. 159–267.

DOLLASE, W. A. (1968) Refinement and comparison of the structures of zoisite and clinozoisite. *Amer. Mineral.* **53,** 1882–1898.

DOLLASE, W. A. (1969). Crystal structure and cation ordering of piemontite. *Amer. Mineral.* **54,** 710–717.

DONNAY, G., AND R. ALLMANN (1968) Si_6O_{10} groups in the crystal structure of ardennite. *Acta Crystallogr.* **B24,** 845–8.

ERNST, W. G., AND C. W. WAI (1970) Mössbauer, infrared, x-ray and optical study of cation ordering and dehydrogenation in natural and heat-treated sodic amphiboles. *Amer. Mineral.* **55,** 1226–1258.

FRONDEL, J. W. (1964) Variation of some rare earths in allanite. *Amer. Mineral.* **49,** 1159–77.

IBERS, J. A. (1962) *International Tables for X-ray Crystallography*, Vol. 3. The Kynock Press, Birmingham, England, Table 3.3.1A.

INGALLS, R. (1964) Electric-field gradient tensor in ferrous compounds. *Phys. Rev.* **133,** A787–A795.

ITO, T. (1950) *X-ray Studies on Polymorphism*. Maruzen Co., Tokyo, Chap. 5.

———, N. MORIMOTO, AND R. SADANAGA (1954) On the structure of epidote. *Acta Crystallogr.* **7,** 53–59.

NEUERBERG, G. J. (1954) *Allanite pegmatite*, San Gabriel Mountains, Los Angeles County, California. *Amer. Mineral.* **39,** 831–834.

PALACHE, C. (1935) The minerals of Franklin and Sterling Hill, Sussex County, New Jersey. *U. S. Geol. Surv. Prof. Pap.* **180,** p. 98.

PENFIELD, S. L., AND C. H. WARREN (1899) Some new minerals from the zinc mines at Franklin, N.J. and note concerning the chemical composition of ganomalite. *Amer. J. Sci. 4th Ser.* **8,** 339–353.

PUDOVKINA, Z. V., AND I. A. PIATENKO (1963) The crystalline structure of non-metamict orthite. *Dokl. Akad. Nauk SSSR* **153,** 695–699.

RUMANOVA, I. M., AND I. M. NIKOLAEVA (1959) Crystal structure of orthite. *Kristallografiya* **4,** 829–835. [Transl. *Sov. Phys.-Crystallogr.* **4,** 789–795 (1959).]

SHANNON, R. D., AND C. T. PREWITT (1969) Effective ionic radii in oxides and fluorides. *Acta Crystallogr.* **B25,** 925–946.

UEDA, T. (1955). The crystal structure of allanite $OH(Ca, Ce)_2(Fe^{3+}Fe^{2+})Al_2OSi_2O_7SiO_4$. *Mem. Coll. Sci. Univ. Kyoto, Ser. B,* **22,** 145–163.

ZACHARIASEN, W. H. (1963). The crystal structure of monoclinic metaboric acid. *Acta Crystallogr.* **16,** 385–389.

Manuscript received, September 10, 1970; accepted for publication, October 15, 1970.